ACS ENVIRONMENTAL Au
AN OPEN ACCESS JOURNAL OF THE AMERICAN CHEMICAL SOCIETY



pubs.acs.org/environau
Article

# Protein-Decorated Reverse Osmosis Membranes with High Gypsum Scaling Resistance

*Published as part of ACS Environmental Au special issue "2024 Rising Stars in Environmental Research".*

Shinyun Park, Xitong Liu, Tianshu Li, Joshua L. Livingston, Jin Zhang, and Tiezheng Tong*

Cite This: ACS Environ. Au 2024, 4, 333−343
Read Online

ACCESS | Metrics & More | Article Recommendations | Supporting Information

**ABSTRACT:** The global challenge of water scarcity has fueled significant interest in membrane desalination, particularly reverse osmosis (RO), for producing fresh water from various unconventional sources. However, mineral scaling remains a critical issue that compromises the membrane efficiency and lifespan. This study explores the use of naturally occurring proteins to develop scaling-resistant RO membranes through an eco-friendly modification method. We systematically evaluate three protein modification techniques, namely, polydopamine (PDA)-assisted coating, protein conditioning, and protein drying, for fabricating membranes resistant to gypsum scaling. Protein conditioning is found to be the most effective approach, resulting in protein-decorated membranes with an exceptional resistance to gypsum scaling. We also demonstrate that a hydrated protein layer is essential for optimal scaling resistance. To further understand the mechanism underlying the scaling resistance of protein-decorated membranes, five proteins (i.e., bovine serum albumin, casein, lactalbumin, lysozyme, and protamine) with distinct physicochemical properties are used to explore the key factors governing membrane scaling resistance. The results of dynamic RO experiments indicate that the molecular weight of proteins plays a crucial role, with higher molecular weights leading to higher membrane scaling resistance through steric effects. However, static experiments of bulk crystallization highlight the importance of electrostatic interactions, where proteins with more negative charge delay gypsum crystallization more effectively. These findings suggest the difference between gypsum scaling in the RO and gypsum crystallization in bulk solutions. Overall, this research offers a novel approach to developing resilient and sustainable RO membranes for the desalination of feedwater with high scaling potential while elucidating mechanistic insights on the mitigating effects of protein on gypsum scaling.

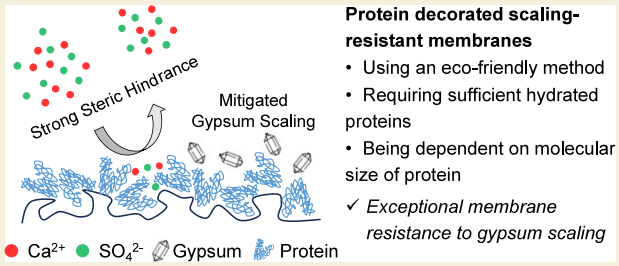


**KEYWORDS:** *gypsum scaling, reverse osmosis, scaling-resistant membrane, membrane modification, protein coating, antiscaling mechanism*

## 1. INTRODUCTION

To cope with the global challenge of water scarcity, membrane desalination, especially reverse osmosis (RO), has garnered significant interest as a promising strategy for producing fresh water from diverse unconventional water sources such as seawater, brackish water, and wastewater.[1−3] However, membrane fouling has been a critical constraint that limits the efficiencies of RO systems, reducing membrane performance and lifespan while increasing operational and maintenance costs.[4−6] Among different types of membrane fouling, mineral scaling (i.e., inorganic fouling), which occurs when the concentrations of scale precursors exceed the solubility of sparingly soluble minerals, has recently received increasing attention.[7,8] Mineral scaling is a problematic issue because the precipitated scales block membrane pores, cause membrane degradation, and consequently reduce the effectiveness of RO process.[4,9,10] Therefore, effective approaches for mitigating mineral scaling are essential to achieving resilient and effective desalination for promoting water sustainability.

Several strategies of scaling mitigation have been adopted in RO desalination including the use of antiscalants, feedwater pretreatment, periodic membrane cleaning, and the fabrication of scaling-resistant membrane.[4,11] Among these options, scaling-resistant membrane is advantageous as it aligns well with current desalination infrastructures and avoids the needs of additional chemicals or procedural steps.[12] However, comparing to a plethora of antifouling membranes against organic and biological fouling,[13−17] there have been only a few

Received: July 22, 2024
Revised: September 18, 2024
Accepted: September 19, 2024
Published: September 30, 2024

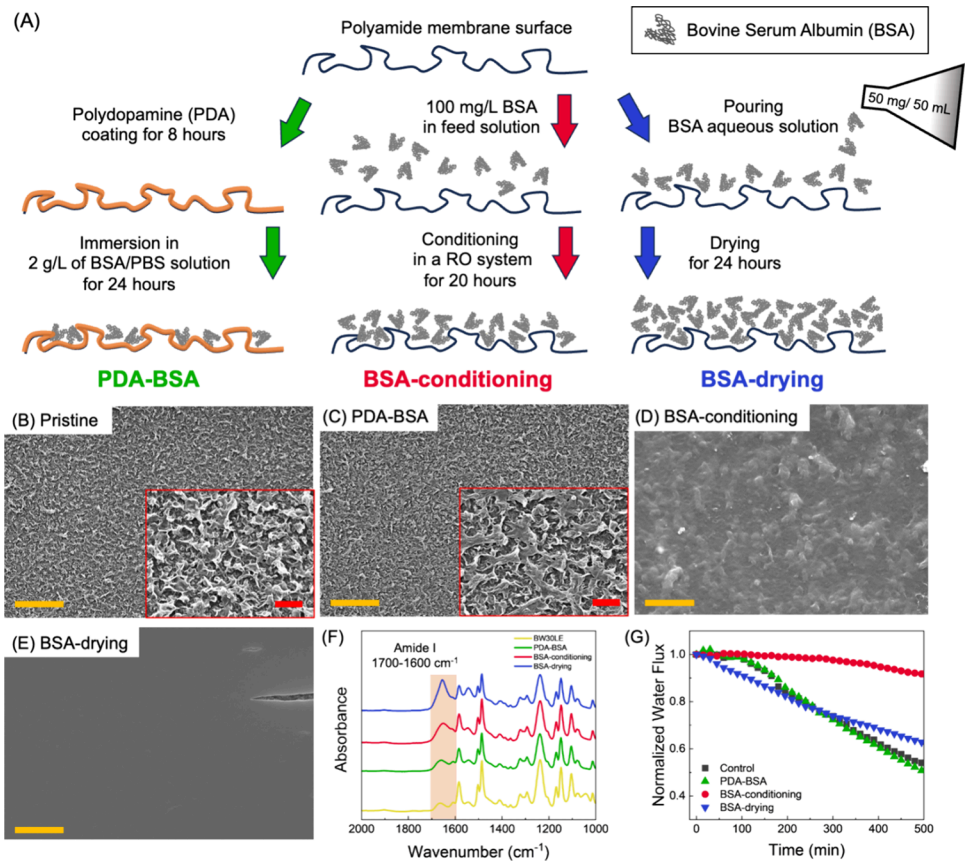


**Figure 1.** (A) Schematics illustrating membrane protein modification methods. Note that BSA was used as a model protein for assessing the modification methods. (B–E) SEM images of the membrane surfaces after protein modification: (B) pristine and BSA-decorated membranes with different methods: (C) PDA-BSA, (D) BSA-conditioning, and (E) BSA-drying membranes. The yellow scale bars and the red scale bars in the inserted images in (B) and (C) represent 10 and 2 $\mu$m, respectively. (F) ATR-FTIR spectra of the pristine and protein-decorated membranes. The highlighted region at 1700–1600 $cm^{-1}$ represents a characteristic peak of proteins (amide I). (G) Normalized water flux behaviors of pristine (i.e., control) and protein-decorated membranes during RO gypsum scaling tests for 500 min.

studies focusing on the development of scaling-resistant membranes.[11,18−20] An example of such studies is the work by Lin et al.,[11] who employed free-radical graft polymerization to modify the RO membrane surface. Polymer brushes were grafted via polymerization of methacrylic acid or acrylamide after plasma activation, with the modified membranes exhibiting reduced gypsum ($CaSO_4{\cdot}2H_2O$) scaling. Jaramillo et al.[20] also utilized atom transfer radical polymerization to graft zwitterionic poly(sulfobetamine methacrylate) on a polyamide membrane surface to improve membrane scaling resistance.

While the literature demonstrates the potential of scaling-resistant membranes to mitigate mineral scaling in RO, existing methods typically involve intricate, multistep processes that increase the complexity and cost of membrane fabrication. Moreover, these methods usually use a variety of hazardous organic chemicals, potentially leading to negative impacts on both the environment and human health. Therefore, pursuing more sustainable and environmentally benign approaches for fabricating scaling-resistant membranes is imperative. In this context, our recent study shows that the coexistence of protein bovine serum albumin (BSA) significantly reduces the extent of gypsum scaling in RO.[21] Inspired by this finding, we hypothesize that the use of naturally occurring proteins in membrane surface modification can be an eco-friendly method of creating novel membranes resistant to gypsum scaling.

In this study, we systematically explored the possibility of developing scaling-resistant RO membranes by using a simple, scalable method of protein modification. We employed three different methods that resulted in RO membranes decorated with proteins of varied quantities, types, and hydration status. The scaling resistances of the modified membranes were examined and compared in dynamic cross-flow gypsum scaling tests of RO. We further investigated the correlation between protein properties and membrane scaling resistance by using a variety of proteins (i.e., BSA, casein, lactalbumin, lysozyme, and protamine). Static experiments in which bulk nucleation of gypsum dominates were also performed to gain a better understanding of the scaling resistance mechanism. Our work provides a new avenue of fabricating scaling-resistant membranes without the use of any synthetic chemicals, having the potential of improving the resilience and sustainability of RO desalination as a more feasible means of augmenting water supply for climate adaptation.

## 2. MATERIALS AND METHODS

### 2.1. Materials

Commercial polyamide RO membranes (BW30LE) were acquired from Dupont FilmTec (Wilmington, Delaware). Calcium chloride dihydrate ($CaCl_2{\cdot}2H_2O$), sodium sulfate ($Na_2SO_4$), sodium hydroxide (NaOH), and hydrochloric acid (HCl) were purchased from Fisher Chemical (Hampton, New Hampshire). Dopamine hydro-


https://doi.org/10.1021/acsenvironau.4c00057
ACS Environ. Au 2024, 4, 333−343

chloride, tris(hydroxymethyl)aminomethane (Tris), phosphate-buffered saline (PBS), 2-propanol (IPA, >99.5%), and proteins (i.e., BSA, lysozyme, lactalbumin, casein, and protamine) were obtained from Sigma-Aldrich (St. Louis, Missouri). Deionized (DI) water (>18.2 MΩ) produced by a water purification system (Millipore, Burlington, Massachusetts) was used for all the experiments.

## 2.2. Membrane Modification Methods

Three different methods were employed to modify the membrane surface with proteins (Figure 1A): (1) polydopamine (PDA)-assisted protein coating, (2) protein conditioning, and (3) protein drying. Before these modification steps, the BW30LE membranes were immersed in a mixture of IPA and DI water (1:1 in a volumetric ratio) to remove impurities and then stored in DI water for modification. For PDA-assisted protein coating, the procedure was adopted from the work by Zhu et al.[22] The PDA layer is known to act as a versatile platform for surface modification due to its reactive groups.[23] In brief, dopamine hydrochloride was dissolved in Tris buffer (10 mM, pH 8.5) to achieve a concentration of 1 g $L^{-1}$. This solution was then immediately poured into the polyamide active layer of the BW30LE membrane to initiate the polymerization reaction. After 8 h, the PDA-coated membrane was thoroughly rinsed with DI water and subsequently immersed in a 2 g $L^{-1}$ protein solution in PBS buffer (10 mM, pH 7.4) at room temperature. Following 24 h of immersion, the modified membrane was rinsed and stored in DI water. The membranes modified with this method will be denoted as "PDA-protein" membrane, in which protein can be referred to BSA, casein, lactalbumin, lysozyme, or protamine. For the protein-conditioning method, the BW30LE membrane was compacted in a lab-scale cross-flow RO system overnight with DI water, and then the feedwater was switched to a 100 mg $L^{-1}$ protein aqueous solution with 10 mM of $CaCl_2{\cdot}2H_2O$ to form a protein layer on the membrane surface. After 20 h of conditioning, the protein-coated membrane was taken out from the membrane cell, gently washed with DI water, and stored in DI water. These membranes will be labeled as "protein conditioning". For the protein-drying method, 1 g $L^{-1}$ of protein aqueous solution was first prepared and then 50 mL of this solution was poured onto a membrane surface clamped onto a glass plate with a frame, which has an inner area of 8 × 11 $cm^2$. After being incubated at room temperature for 24 h to allow water to fully evaporate, the membrane was taken apart from the frame and stored in DI water for further use. The membranes modified using this method will be referred to as "protein-drying" membrane.

## 2.3. Membrane Performance Evaluation

The performance of the pristine BW30LE membrane and membranes modified with proteins (i.e., BSA, casein, lactalbumin, lysozyme, protamine) was assessed in an RO system with an effective membrane area of 20 $cm^2$.[24] For all the tests, the RO system was operated at a cross-flow velocity of 21.3 cm $s^{-1}$ and a temperature of 22 ± 1 °C, with the pH of the feedwaters adjusted to 6.5 ± 0.1 using 1 M HCl and 1 M NaOH solutions. After an overnight compaction step with DI water at 220 psi, the pure water flux was measured under the same pressure to calculate the water permeability coefficient. Then, the salt rejection of each membrane was measured with a 20 mM NaCl solution. Subsequently, to induce gypsum scaling for evaluating membrane scaling resistance, the feedwater was changed to a gypsum-saturated solution containing 24 mM $CaCl_2{\cdot}2H_2O$ and 24 mM $Na_2SO_4$ with a saturation index (SI) of 0.39. The SI, defined as ln $IAP/K_{sp}$ (where IAP represents ion activity products and $K_{sp}$ represents the solubility equilibrium constant), was calculated by the PHREEQC software. The initial permeate water flux was 30 ± 3 L $m^2$ $h^{-1}$ (LMH) for all the membranes and monitored for 500 min during the scaling tests using a digital flow meter (FlowCal 5000, Tovatech, Plano, Texas). The recorded flux data were then normalized with respect to the initial value for comparison. After the gypsum scaling tests, the membrane coupons were gently washed with DI water and stored for characterizations after drying under ambient conditions.

## 2.4. Static Experiments of Gypsum Crystallization in Bulk Solutions

Static experiments were conducted to examine gypsum crystallization in bulk solutions with different proteins (i.e., BSA, casein, lactalbumin, lysozyme, and protamine). For the control group (i.e., without proteins), separately prepared solutions of $CaCl_2{\cdot}2H_2O$ and $Na_2SO_4$ solutions were mixed with a magnetic stirrer, achieving a final mixture containing 42 mM of gypsum precursors and an SI of 1.08. A higher concentration of scalants was used compared to the dynamic experiments, in order to ensure that gypsum crystallization could be observed within a reasonable time frame. For the experimental groups, proteins were introduced to the gypsum-saturated solutions at a concentration of 20 mg $L^{-1}$. This concentration was selected based on our previous study, which reported that it was sufficient to exhibit the effects of protein on gypsum crystallization in the bulk solution.[21] The pH of the solution was adjusted to 6.5 ± 0.1 using 1 M NaOH or 1 M HCl solutions, and the solution conductivity was monitored using a conductivity meter (CON2700, Oakton, Vernon Hills, Illinois). The conductivity of the solutions decreased over time after an induction period, indicating gypsum crystallization that consumes $Ca^{2+}$ and $SO_4^{2-}$ ions. Once equilibrium was reached, which was evidenced by a stable conductivity, the formed precipitates were collected via vacuum filtration using 2.5 μm filter papers (Grade 5, Whatman, Maidstone, UK), air-dried, and stored under ambient conditions for further analyses.

## 2.5. Characterization of Membranes, Gypsum Scales, and Proteins

The pristine and protein-decorated membranes before and after gypsum scaling were characterized by using several techniques. The morphologies of gypsum scales and the membrane surfaces were analyzed by scanning electron microscopy (SEM, JEOL JSM-6200F) with a 15 nm gold coating. The crystalline structure of the scale layer after gypsum scaling was analyzed via X-ray diffraction (XRD, Bruker D8 Discover DaVinci). The XRD patterns were recorded for an angular range from 5 to 60°, with X-ray generation at the voltage and current of 40 mV and 40 mA, respectively. A contact angle goniometer (KRÜSS DSA10 Drop Shape Analysis System, KRÜSS Scientific, Germany) was used to measure the water contact angle of the membranes via a sessile drop method. The zeta potentials of the pristine and protein-decorated membranes were measured by employing an electrokinetic analyzer with an adjustable gap cell (SurPASS, Anton-Paar, Graz, Austria). The measurements were conducted using 1 mM KCl as the background electrolyte, with the pH value adjusted between 2 and 10 by titration with 0.1 M HCl and 0.1 M KOH solutions. To measure the zeta potential of the proteins, aqueous protein solutions were prepared at a concentration of 100 mg $L^{-1}$, and the solution pH was adjusted to 6.5 ± 0.1. The zeta potential measurements were then conducted by using a Malvern Zetasizer Nano ZS (Malvern Panalytical Ltd., UK).

Furthermore, attenuated total reflection-Fourier transform infrared (ATR-FTIR) spectroscopy (Nicolet iS50 spectrometer, Thermo Fisher Scientific) was employed to characterize the membrane surface functionality and protein structures. The ATR-FTIR spectra of the membranes were obtained with 32 scans of each sample at a wavelength range from 4000 to 550 $cm^{-1}$. For investigating the effect of hydration on secondary structure of proteins, the amide I peak (1700−1600 $cm^{-1}$) of protein was analyzed as reported by the literature.[25] Briefly, a BSA aqueous solution (1 g $L^{-1}$ BSA, representing the hydrated form of BSA), dried BSA powder (representing the dehydrated form of BSA), and DI water were used as samples for collecting the FTIR spectra. The samples were scanned 256 times, and the obtained spectra within the range 1700−1600 $cm^{-1}$ were analyzed by employing the peak resolve function equipped in OMNIC software.[26] Using the dried BSA powder ensured that the observed peaks were only associated with dehydrated protein. For the BSA aqueous solution, we were able to obtain peaks associated with hydrated protein by subtracting the peaks associated with DI water from those of the BSA aqueous solution. Furthermore, we did not use BSA-decorated membranes for this analysis because


https://doi.org/10.1021/acsenvironau.4c00057
ACS Environ. Au 2024, 4, 333−343

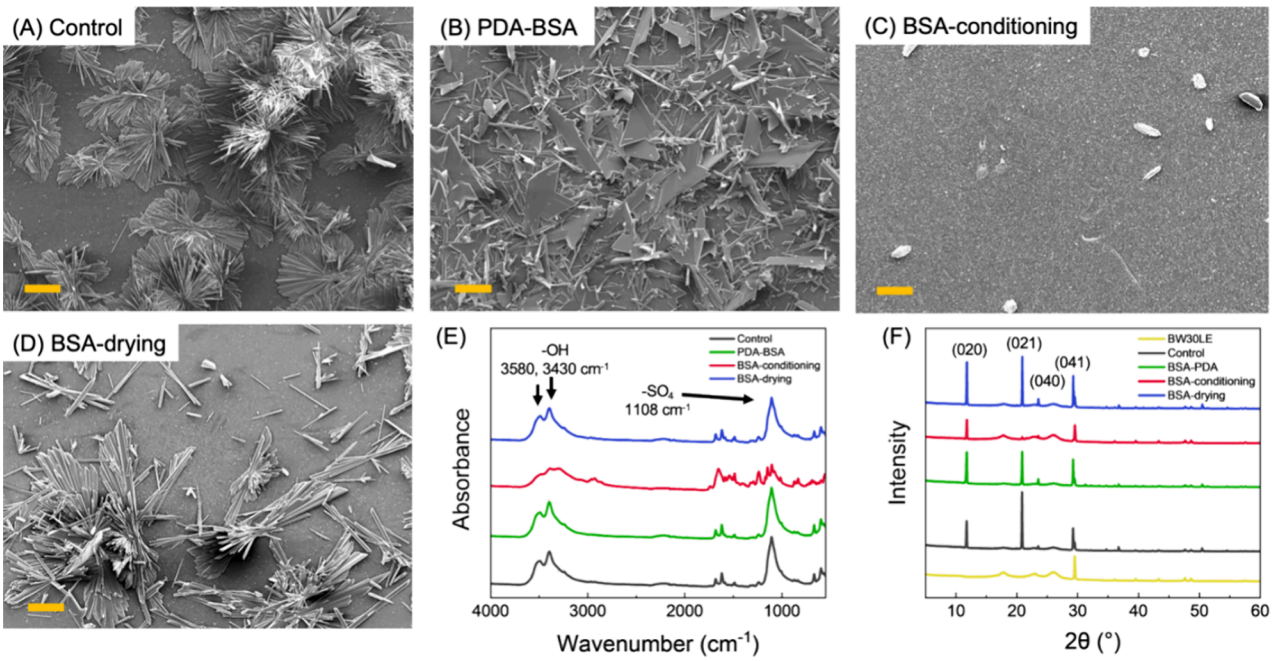


**Figure 2.** (A–D) SEM images of the membrane surfaces after gypsum scaling on (A) a pristine BW30LE membrane (control), (B) a PDA-BSA membrane, (C) a BSA-conditioning membrane, and (D) a BSA-drying membrane. The yellow scale bars represent 100 $\mu$m. (E, F) Spectra of the membrane surfaces after gypsum scaling obtained using (E) ATR-FTIR and (F) XRD.

(1) the thickness of the BSA layer on the membrane surface after modification varied between BSA-conditioning and BSA-drying approaches, which would affect the FTIR spectra, and (2) there is an overlap in amide peaks of FTIR spectra between the polyamide layer of the RO membrane and proteins.

## 3. RESULTS AND DISCUSSION

### 3.1. Comparison of Protein Coating Methods

In this section, we primarily focused on BSA to evaluate the effectiveness of three protein coating methods, due to our previous finding that the coexistence of BSA effectively mitigates gypsum scaling in RO.[21] Prior to the gypsum scaling tests, the BSA-coated membranes fabricated by different methods (as described in Figure 1A) were characterized. As displayed by top-view SEM images, the surface of the pristine BW30LE membrane exhibited a typical ridge-and-valley structure of the polyamide layer (Figure 1B, and its inset image), while a BSA layer fully covered the membrane surface in the case of the BSA-conditioning and BSA-drying membranes (Figure 1D,E). However, such a BSA layer was not observed when the PDA-BSA method was used, although a noticeable difference between the PDA-BSA membrane and the pristine BW30LE membrane was observed at a higher magnification (Figure 1C and its inset image). The presence of a BSA layer on the modified membranes was further confirmed via ATR-FTIR analysis (Figure 1F). The characteristic band of protein at the range of 1700−1600 $cm^{-1}$ (amide I, N−C−O)[27] was significantly intensified for the BSA-conditioning and BSA-drying membranes while it was slightly enhanced for the PDA-BSA membrane. This is consistent with the results of SEM observations, demonstrating that BSA was successfully grafted on the membrane surface, but the PDA-BSA method led to a lesser grafting density than the other two methods.

The BSA-decorated membranes were tested in RO gypsum scaling tests to assess their scaling resistance. As shown in Figure 1G and Figure S1 (Supporting Information), the water flux of the pristine membrane decreased by ∼50% after 500 min due to gypsum scaling, which was comparable to that for the PDA-BSA membrane. In contrast, the BSA-conditioning membrane displayed exceptional scaling resistance, with a minor water flux decline of only ∼10% during the same period. These results indicate that (1) coating BSA on the membrane surface can successfully mitigate gypsum scaling in RO and (2) to pose a mitigating effect on gypsum scaling, the decorated BSA layer should cover the membrane surface with sufficient protein quantity. However, despite the higher amount of BSA coated on the surface, the BSA-drying membrane showed a negligible improvement in scaling resistance compared to the pristine membrane. This result suggests that the hydration status of the protein layer might play a role in regulating membrane scaling resistance, which will be further discussed Section 3.2.

After the gypsum scaling RO tests, the scaled membranes were analyzed with several characterization techniques. The SEM images of the membrane surface revealed that the crystal morphology of gypsum was altered on the PDA-BSA membrane (Figure 2B) when compared to the rosette-shaped gypsum crystals on the pristine membrane (Figure 2A). Thus, although the PDA-BSA membrane did not mitigate gypsum scaling (Figure 1G), the moderate amount of grafted BSA was able to interrupt gypsum crystallization and consequently change the morphology of gypsum. Furthermore, a significant difference was noticed on the BSA-conditioning membrane, where the gypsum crystal formation was remarkably inhibited, and only a few rod-shaped crystals were observed (Figure 2C). However, there was no clear morphological alteration regarding gypsum formed on the BSA-drying membrane (Figure 2D), despite a thick BSA layer covering the membrane surface. This result is consistent with the water flux results (Figure 1G) and supports our hypothesis that the protein hydration status is an important factor of the mitigating effect of protein on gypsum scaling. In addition, the membrane


https://doi.org/10.1021/acsenvironau.4c00057
ACS Environ. Au 2024, 4, 333−343

surfaces were further analyzed with ATR-FTIR spectroscopy. As shown in Figure 2E, strong gypsum characteristic peaks (i.e., 3580 and 3430 $cm^{-1}$ for −OH and 1108 $cm^{-1}$, respectively, for $-SO_4$)[28] were observed for all membranes after gypsum scaling, except for the BSA-conditioning membrane that showed both BSA characteristic peaks (i.e., 1700−1600 $cm^{-1}$, attributed to amide I bond, N−C−O)[27] and moderate gypsum peaks. These results are consistent with the SEM observations, where the formation of gypsum crystals was significantly hindered on the BSA-conditioning membrane.

Furthermore, XRD was employed to probe the crystalline structure of the gypsum scales formed on the membrane surfaces (Figure 2F). The characteristic peaks of gypsum crystals, corresponding to the (020), (021), (040), and (041) facets,[29] were observed for all of the membranes after scaling tests, indicating the presence of gypsum scales. However, when the spectra were examined more closely by looking at the peak intensity ratio of (020) to (021) facets, changes were observed for the BSA-decorated membranes compared to the pristine membrane. For example, the ratios associated with gypsum crystals on the PDA-BSA and BSA-drying membranes were moderately increased from 0.5 (for the pristine membrane) to 1.0 and 0.9, respectively, demonstrating a noticeable but not pronounced alteration of crystalline structure. However, the peak intensity ratio was significantly increased to 3.7 in the case of the BSA-conditioning membrane, majorly due to a significant decrease of the peak intensity for the (021) facet. This result suggests that the BSA layer formed by the protein-conditioning method greatly interrupted the crystallization of gypsum by preventing its growth in certain orientations (e.g., along the (021) facet), which is consistent with the observation in our previous study[21] and explains the exceptional scaling resistance of the BSA-conditioning membrane. In addition, the distinct difference in the XRD spectra between BSA-conditioning and BSA-drying membranes provides additional evidence of the importance of protein hydration status in the interruption of gypsum crystallization by BSA. As a result, the protein-conditioning method was found to be the best option to fabricate BSA-decorated scaling-resistant RO membranes, and this method was applied to most experiments relating to the next sections.

### 3.2. Importance of Hydration Status of the Protein Layer

To further understand the role of protein hydration status in regulating the scaling resistance of BSA-decorated membranes, we performed an additional set of gypsum scaling experiments with two more membranes: (1) a BSA-conditioning membrane after drying for 2 days under ambient conditions (denoted as the "BSA-conditioning-dried" membrane) and (2) a BSA-drying membrane after rewetting by immersing the membrane in DI water for 2 days (denoted as "BSA-drying-wet" membrane). As shown in Figure 3 and Figure S1, the scaling resistance of the BSA-conditioning membrane was greatly reduced after being dried, while rewetting did not considerably improve the scaling resistance of the BSA-drying membrane. These results confirm that hydrated proteins are necessary for the BSA-decorated membrane to possess a high scaling resistance. Once the proteins are dehydrated, the antiscaling efficiency of the BSA-decorated membrane is significantly compromised and cannot be restored by simply wetting the membrane surface. These findings are further supported by SEM images of the membrane surfaces after gypsum scaling (Figure S2, Supporting Information). Although gypsum

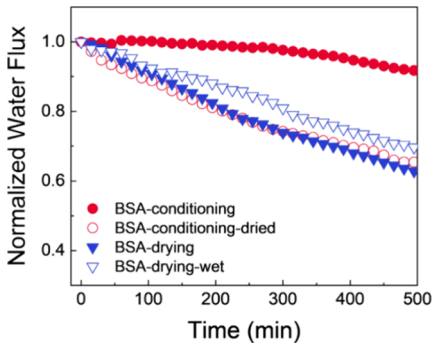


**Figure 3.** Normalized water flux curves of RO using different BSA-decorated membranes during gypsum scaling tests for 500 min. To see the effect of protein hydration, the BSA-conditioning membrane was air-dried (labeled as "BSA-conditioning-dried") and the BSA-drying membrane was immersed in DI water (labeled as "BSA-drying-wet") for 2 days before the gypsum scaling tests.

formation was greatly hindered on the surface of the BSA-conditioning membrane after 500 min of gypsum scaling (Figure S2A), rosette-like gypsum crystals appeared on the surface of the BSA-conditioning-dried membrane. After rewetting, the surface of BSA-drying-wet membrane was also subject to the formation of rosette-like gypsum scales (Figure S2D), similar to what was experienced by the BSA-drying membrane (Figure S2B). Such observations of gypsum crystal morphologies provide additional evidence that the BSA layer loses its ability to hinder gypsum scaling after dehydration, which is irreversible.

To further scrutinize the impact of dehydration on the protein layer, the secondary structure of the protein was analyzed via ATR-FTIR. The result of peak deconvolution for the FITR spectra reveals that compared to the spectra of the hydrated form of BSA, the peak for the $\alpha$-helix was reduced and the peak for the $\beta$-sheet was enhanced for the dehydrated form of BSA (Figure S3, Supporting Information). This alteration provides evidence that protein dehydration as a result of drying leads to protein denaturation that involves the loss of native structure of the protein. The decrease in helicity of the protein turns the protein molecule into an unfolded shape, and it has been reported that an unfolded shape of protein resulted in a denser layer than the native form.[30] This is because unfolded proteins render buried sites exposed, leading to more protein−protein interactions.[31] A denser layer of dehydrated proteins is evidenced by the water permeability of the membranes, as displayed in Figure S4 (Supporting Information). The water permeability coefficient of the BSA-conditioning membrane was 5.2 LMH $bar^{-1}$. However, after the BSA-conditioning membrane was dried, the water permeability coefficient of the BSA-conditioning-dried membrane dramatically dropped to 1.5 LMH $bar^{-1}$, which was similar to that of the BSA-drying membrane. These results further support the statement that protein dehydration causes structural alteration, which is likely responsible for the important role of protein hydration status in regulating the scaling resistance of protein-decorated membranes.

### 3.3. Relating Protein Properties to Membrane Scaling Resistance

To explore which protein properties contribute to the antiscaling effect on gypsum scaling, various proteins, including casein, lactalbumin, lysozyme, and protamine, were used to fabricate protein-decorated membranes in addition to BSA.


https://doi.org/10.1021/acsenvironau.4c00057
ACS Environ. Au 2024, 4, 333−343

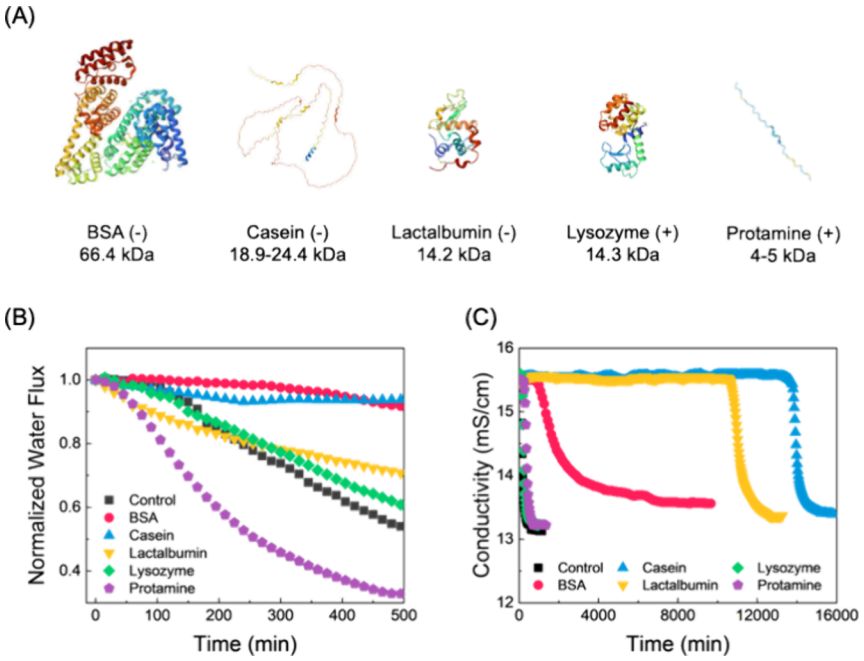


**Figure 4.** (A) Molecular structures of proteins used in this study. The 3D structures of BSA (ID: 3V03), casein (CSM (Computed Structure Models): AF_AFP28550F1), lactalbumin (ID: 1A4B), lysozyme (ID: 253L), and protamine (CSM: AF_AFP69014F1) were obtained from the Protein Data Bank (RCSB database, http://www.rcsb.org). The charge of the protein at near neutral pH was labeled as (+) and (−) for positively and negatively charged proteins, respectively. (B) Normalized water fluxes of protein-decorated membranes during the RO gypsum scaling tests for 500 min. The labels for each protein represent the corresponding protein-decorated membrane, while "Control" indicates the pristine membrane. (C) Solution conductivity as a function of time for a gypsum-saturated solution in the absence (Control) and presence of proteins. The labels for each protein indicate the conditions under which the solution contains the corresponding protein in addition to gypsum scalants.

These proteins possess different physicochemical properties such as molecular structure, molecular weight, and surface charge. As shown in Figure 4A, the molecular structures of these proteins differ, exhibiting distinct secondary and tertiary structures due to variations in the number and types of constituting amino acids. Such structural variations result in changes in protein properties such as molecular size and charge. The molecular weights of BSA, casein, lactalbumin, lysozyme, and protamine are 66.4, 18.9−24.4, 14.2, 14.3, and 4−5 kDa, respectively.[32−34] At near neutral pH, BSA, casein, and lactalbumin are negatively charged, whereas lysozyme and protamine are positively charged (Figure S5A, Supporting Information).

The protein-conditioning method was used to decorate the membrane surface with proteins, because this method resulted in the best membrane scaling resistance, as described in Sections 3.1 and Section 3.2. During the 20 h protein-conditioning step, the water flux of RO decreased due to the deposition of proteins onto the membrane surface (Figure S5B, Supporting Information). Casein and lactalbumin led to the most significant reductions in water flux, whereas the water flux during lysozyme and BSA conditioning slightly decreased. These results indicate that the amount of proteins in the coated layer was likely to vary depending on the protein type. The water permeability coefficients of the protein-decorated membranes generally followed the order of final water flux of the conditioning step (Figure S5C, Supporting Information), except that the lactalbumin-conditioned membrane exhibited a relatively high water permeability despite significant water flux reduction during lactalbumin conditioning. This phenomenon was due to the partial detachment of the lactalbumin layer during gentle rinsing with DI water after the conditioning step (Figure S6, Supporting Information).

The surface properties of the protein-decorated membranes were analyzed comprehensively. As shown in Figure S7A−E (Supporting Information), SEM analysis reveals that the surfaces of all the protein-decorated membranes were covered by a protein layer after the conditioning step, as evidenced by the absence of the characteristic ridge-and-valley structure of the polyamide layer observed for the pristine BW30LE membrane (Figure 1B). In the case of the lactalbumin-decorated membrane (Figure S7C), the protein layer remained present despite partial detachment during DI water rinsing after the conditioning step. This infers that a sufficient amount of proteins remained firmly on the membrane surface to cover the polyamide layer. When examining the characteristic peak of proteins (amide I, 1700−1600 $cm^{-1}$) in the FTIR spectra (Figure S7F), this peak was intensified for all of the protein-decorated membranes compared to the pristine membrane. However, the extent of such intensification varied with the protein type, which suggests that the amount of proteins differed and is consistent with different water permeability coefficients (Figure S5C). Furthermore, the water contact angles of the membranes were measured to assess their hydrophilicity. As shown in Figure S5D, the contact angles of the protein-decorated membranes were higher than those of the pristine membrane, indicating that the protein layer made the membrane surface less hydrophilic to varying extents, depending on the protein type.

These protein-decorated membranes were subjected to gypsum scaling tests to evaluate their scaling resistance. As shown in Figure 4B and Figure S8A (Supporting Information), the membranes exhibited distinct flux behaviors in the


https://doi.org/10.1021/acsenvironau.4c00057
ACS Environ. Au 2024, 4, 333−343

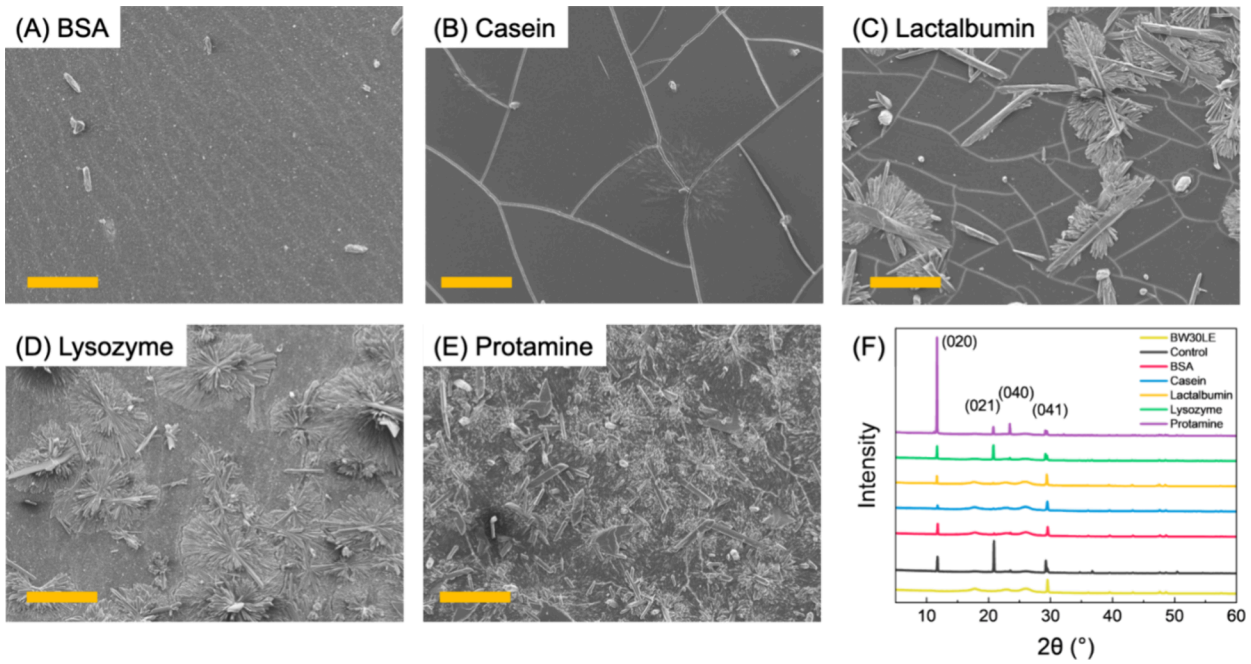


**Figure 5.** (A–E) SEM images of the membrane surface after gypsum scaling in RO for (A) BSA-, (B) lysozyme-, (C) lactalbumin-, (D) casein-, and (E) protamine-decorated membranes. (F) XRD patterns of gypsum scales on the protein-decorated membranes.

presence of gypsum scaling. Specifically, BSA- and casein-decorated membranes showed the best scaling resistance that retained approximately 90% of the initial water flux after 500 min of operation, which are better than or comparable to the other antiscaling membranes reported in the existing literature where synthetic chemicals were involved in membrane fabrication (Table S1, Supporting Information). In contrast, membrane coating by lactalbumin and lysozyme did not result in significant mitigation of gypsum scaling, with the lactalbumin- and lysozyme-decorated membranes having slightly higher final fluxes than that of the pristine BW30LE membrane (i.e., control). Meanwhile, protamine-decorated membranes experienced a significant decline of water flux, with a final flux of only ∼36% of the initial flux, which was much lower than that of the control membrane (∼58%). Thus, protamine coating did not reduce but accelerated gypsum scaling. These results highlight the varying effects of different protein coatings on gypsum scaling in RO desalination.

The SEM observation of the scaled membrane surfaces (Figure 5A–E) further supports this conclusion with the amount of gypsum scales observed on the membrane surfaces aligned with the scaling resistance results (Figure 4B). In detail, only a few gypsum particles were observed on BSA- and casein-decorated membranes, consistent with the high scaling resistance of these membranes. However, more gypsum scales were seen on the surface of lactalbumin- and lysozyme-coated membranes, while a substantially higher number of gypsum crystals were found to form on the protamine-coated membrane. We further characterized the gypsum scales by XRD analysis. As shown in Figure 5E, although all of the membranes exhibited the characteristic peaks of gypsum crystals (i.e., corresponding to the (020), (021), (040), and (041) facets), the intensity of each peak varied depending on the protein type, and all of the protein-coated membranes exhibited an enhanced (020)/(021) peak intensity ratio compared to the control (Table S2, Supporting Information). For example, the peak intensity ratio of the protamine-decorated membrane markedly increased from 0.5 (for the pristine BW30LE membrane) to 10.9, driven by the intensified peak of the (020) facet and the diminished peak of the (021) facet. However, the lysozyme-decorated membrane showed only a slight enhancement in the peak intensity ratio (i.e., increasing to 0.9). These findings indicate that protein coating can affect gypsum crystallization by disrupting the growth of gypsum crystals along the (021) facet and redirecting their growth predominantly to the (020) facet, but to different extents depending on the protein type. The alteration in the gypsum characteristic peaks of (020) and (021) facets by proteins is similar to the inhibiting effects of antifreeze proteins on ice crystal growth by binding to a specific facet of ice crystals.[35,36]

In addition, we performed a set of static experiments to investigate the effect of proteins on gypsum crystallization in bulk solution. As observed in Figure 4C and Figure S8B, the conductivity of the gypsum-saturated solution in the absence of protein started to decrease at 68 min, which represents an induction time of gypsum formation that consumes scalant ions (i.e., $Ca^{2+}$ and $SO_4^{2-}$). However, the induction times of the solution in the presence of protein were postponed to 904 min (BSA), 11,570 min (casein), 8525 min (lactalbumin), 110 min (lysozyme), and 207 min (protamine). The phenomenon of delayed induction time in the presence of proteins is consistent with the literature where the presence of organic matter (e.g., humic substances, polysaccharides, and proteins) deferred the induction time of gypsum crystallization in gypsum-saturated solutions.[21,37,38] Nonetheless, it is intriguing that the extent of the delay in induction time varied depending on the protein type, with the order of delay following casein > lactalbumin > BSA > protamine > lysozyme. However, such an order obtained from the static experiments is not in accordance with the order of scaling resistance of protein-decorated membranes shown in the dynamic RO experiments (i.e., BSA = casein > lactalbumin = lysozyme > protamine, Figure 4B). This discrepancy was likely due to the differences between


https://doi.org/10.1021/acsenvironau.4c00057
ACS Environ. Au 2024, 4, 333–343

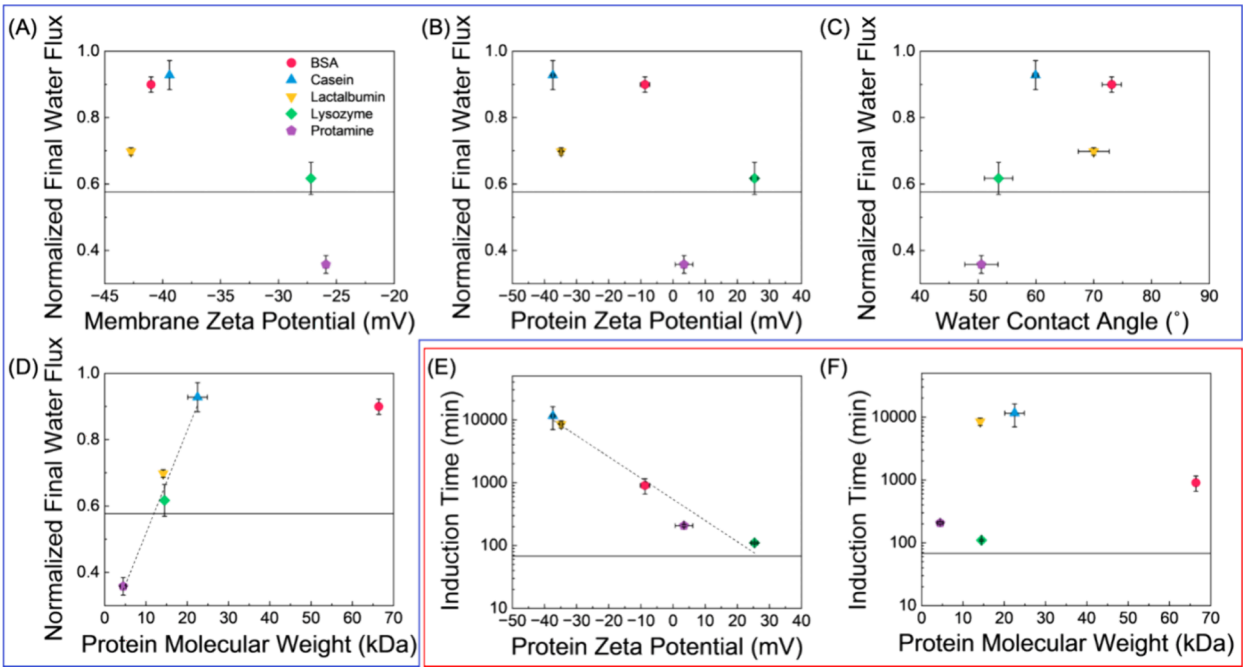


**Figure 6.** Relating gypsum scaling during dynamic and static experiments to the properties of protein and protein-decorated membranes: (A–D, in blue box, dynamic experiment) normalized final water flux versus (A) membrane zeta potential, (B) protein zeta potential, (C) water contact angle, and (D) protein molecular weight. (E, F, in red box, static experiment) Induction time of gypsum crystallization as a function of (E) protein zeta potential and (F) protein molecular weight. Black horizontal lines represent the values from the control group (i.e., in the absence of proteins). The error bars represent one standard deviation and were calculated from triplicate measurements, except for protein molecular weight whose error bars are derived from the values reported in the literature (e.g., casein: 18.9–24.4 kDa, and protamine: 4–5 kDa).[32−34]

surface-initiated and bulk gypsum crystallization, which are influenced by different protein properties. Therefore, it is essential to perform further investigations to understand which specific properties influence the effects of proteins on gypsum scaling in dynamic and static experiments.

As a result, we correlate the properties of both protein-decorated membranes and proteins to their mitigating effects on the gypsum scaling (Figure 6). The correlations between membrane/protein properties and scaling resistance (manifested by normalized final water flux) of the protein-decorated membranes for the dynamic RO experiments are shown in Figure 6A–D. When examining the relationship between membrane zeta potential and the normalized final water flux after gypsum scaling tests (Figure 6A), the membrane scaling resistance generally increases with more negative surface charge, but this correlation does not apply to the lactalbumin-decorated membrane, suggesting the existence of other factors affecting scaling resistance. Furthermore, no clear relationship was observed between protein zeta potential (i.e., protein charge) and membrane scaling resistance or between water contact angle and membrane scaling resistance (Figure 6B,C). Nevertheless, as shown in Figure 6D, the membrane scaling resistance in the dynamic RO experiments appears to be strongly related to the molecular weight of the protein. As the molecular weight of protein increases, membrane scaling resistance becomes higher until a critical molecular weight is reached (18.9–24.4 kDa for casein in this study). This correlation suggests that the mechanism of membrane scaling resistance endowed by protein coating is likely due to the steric hindrance imparted by protein molecules, rather than electrostatic interactions (between scalants and membrane) or the hydrophilicity of protein layers on the membrane surface. Our finding provides additional evidence that steric effects play a key role in protein–gypsum interaction.[39] During dynamic RO experiments, surface-induced crystallization was found to dominate the gypsum scaling process.[21] Therefore, gypsum scaling is effectively hindered when large protein molecules physically block the active areas of the membrane surface where nucleation and crystal growth occur. This hypothesis is supported by findings in our previous study,[21] which showed that amino acids, the building blocks of proteins, did not have any effect on gypsum scaling. Interestingly, we notice that protamine facilitates gypsum scaling in contrast to the mitigating effect observed for the other four proteins. Although we acknowledge that such a facilitating effect needs further investigation to understand its mechanism, it is analogous to a reported study demonstrating that the major difference between antifreeze proteins (which inhibit ice crystal growth) and ice nucleation promoters (which trigger the formation of new ice crystals) is their molecular size.[40] Overall, the results above infer that the molecular size of the protein might be the most important property that regulates the scaling resistance of protein-decorated membranes, while membrane surface charge also plays a role.

In the case of static experiments, electrostatic interactions between scalants and proteins were found to govern gypsum crystallization in the bulk solution (Figure 6E), as evidenced by the strong correlation between the charge of the protein and induction time of gypsum. The induction time of gypsum is prolonged when the charge of protein (manifested by protein zeta potential) becomes more negative. This is likely because the negatively charged moieties of proteins attract calcium ions, leading to the formation of strong protein–calcium complexes. Such an interaction reduces the free calcium ions available in the bulk solution for gypsum crystallization, as similarly described in the literature.[41] However, no relationship


https://doi.org/10.1021/acsenvironau.4c00057
ACS Environ. Au 2024, 4, 333–343

is observed with the molecular weight of the protein (Figure 6F), which is different from what is found for dynamic RO experiments. These findings demonstrate that results of gypsum crystallization in the bulk solution do not predict those of gypsum scaling in dynamic membrane desalination. This difference, which was also reported by our recent work,[21] indicates that gypsum crystallization in the bulk solution is unlikely to be the dominant mechanism of gypsum scaling in RO. Rather, surface-induced nucleation and crystallization are likely to play a more important role.

## 4. CONCLUSIONS

Our study demonstrates the promising potential of using naturally occurring proteins to develop scaling-resistant RO membranes, offering an eco-friendly alternative to the existing methods. We systematically explored three different membrane modification methods (i.e., PDA-assisted coating, protein conditioning, and protein drying) and evaluated the efficiencies of the resultant membranes in mitigating gypsum scaling in RO. Additionally, we tested five proteins (BSA, casein, lactalbumin, lysozyme, and protamine) to identify which physicochemical properties contribute to scaling resistance. The key conclusions of this study include: (1) The protein-conditioning approach was found to be the most effective, resulting in protein-decorated membranes with sufficient proteins for exceptional resistance to gypsum scaling. (2) Maintaining the hydration status of protein is crucial for effective scaling resistance. (3) The scaling resistance of protein-decorated membranes is a function of protein type. The membrane scaling resistance is primarily influenced by the molecular size of the proteins, with the membrane surface charge also playing a role. Therefore, to achieve high membrane resistance to gypsum scaling in RO, a hydrated layer of proteins with a high molecular weight and negative charge is needed. Our study demonstrates that RO membranes with high resistance to gypsum scaling can be successfully fabricated by protein decoration, and such protein-decorated membranes have great potential to extend the lifetime of RO membranes and/or reduce the needs of chemical additions (in pretreatment or as antiscalants) for scaling mitigation.

Nonetheless, further investigations are still needed to fully harness the potential of protein-decorated membranes in improving the RO performance. For example, although the protein-conditioning method reported in this study results in RO membranes with exceptional scaling resistance, further optimization of the protein-conditioning process, such as optimizing the conditioning duration and protein concentration, might lead to better scaling resistance of protein-decorated membranes fabricated with a more efficient and economical manner. Furthermore, while the protein-decorated membranes show promise of mitigating gypsum scaling in RO in this study, their effectiveness against other types of mineral scaling, such as silica scaling that forms via different mechanisms,[42] would need to be verified via separation investigations. Future research should explore the performance of protein-decorated membranes in feedwaters containing other scaling types to fully understand their potential in broader applications. In addition, although this work focuses on proving the concept of mitigating gypsum scaling by protein-decorated RO membranes, the long-term performance of these membranes requires further investigation. Such an effort could be achieved by conducting experiments over extended operational periods or after several cycles of desalination.

## ASSOCIATED CONTENT

### Supporting Information

The Supporting Information is available free of charge at https://pubs.acs.org/doi/10.1021/acsenvironau.4c00057.

Details on normalized final water fluxes with error bars after gypsum scaling for pristine and protein-decorated membranes fabricated with various modification methods; SEM images of membrane surfaces after gypsum scaling; FTIR spectral deconvolution for BSA under different conditions; properties of protein-modified membranes, including water permeability coefficients, zeta potentials, normalized water fluxes during conditioning, and contact angles; photographic evidence of protein detachment from lactalbumin-conditioned membranes; SEM images and ATR-FTIR spectra for membranes modified with different proteins; comparisons of membrane performance with literature data; ratios of the (020)/(021) facets of XRD peak intensities for protein-decorated membranes (PDF)

## AUTHOR INFORMATION


### Corresponding Author

**Tiezheng Tong** − *Department of Civil and Environmental Engineering, Colorado State University, Fort Collins, Colorado 80523, United States; School of Sustainable Engineering and the Built Environment, Arizona State University, Tempe, Arizona 85287, United States;* orcid.org/0000-0002-9289-3330; Phone: +1(970)491-1913; Email: tiezheng.tong@colostate.edu

### Authors

**Shinyun Park** − *Department of Civil and Environmental Engineering, Colorado State University, Fort Collins, Colorado 80523, United States; School of Sustainable Engineering and the Built Environment, Arizona State University, Tempe, Arizona 85287, United States;* orcid.org/0000-0002-0618-8118

**Xitong Liu** − *Department of Civil and Environmental Engineering, George Washington University, Washington 20052, United States;* orcid.org/0000-0002-5197-3422

**Tianshu Li** − *Department of Civil and Environmental Engineering, George Washington University, Washington 20052, United States;* orcid.org/0000-0002-0529-543X

**Joshua L. Livingston** − *Department of Civil and Environmental Engineering, Vanderbilt University, Nashville, Tennessee 37212, United States*

**Jin Zhang** − *Department of Civil and Environmental Engineering, Vanderbilt University, Nashville, Tennessee 37212, United States*

Complete contact information is available at: https://pubs.acs.org/10.1021/acsenvironau.4c00057


### Author Contributions

CRediT: **Shinyun Park** conceptualization, data curation, formal analysis, methodology, validation, visualization, writing - original draft, writing - review & editing; **Xitong Liu** methodology, validation, writing - review & editing; **Tianshu Li** methodology, validation, writing - review & editing; **Joshua**



https://doi.org/10.1021/acsenvironau.4c00057
ACS Environ. Au 2024, 4, 333−343

**Lebron Livingston** data curation; **Jin Zhang** data curation; **Tiezheng Tong** conceptualization, methodology, project administration, resources, supervision, validation, writing - review & editing.

### Notes

The authors declare no competing financial interest.

## ■ ACKNOWLEDGMENTS

This material is based upon work supported by the National Science Foundation under Grant Nos. 2143970 and 2143508.

## ■ REFERENCES

(1) Elimelech, M.; Phillip, W. A. The future of seawater desalination: Energy, technology, and the environment. *Science* **2011**, *333* (6043), 712−717.
(2) Greenlee, L. F.; Lawler, D. F.; Freeman, B. D.; Marrot, B.; Moulin, P. Reverse osmosis desalination: water sources, technology, and today's challenges. *Water Res.* **2009**, *43* (9), 2317−2348.
(3) Shenvi, S. S.; Isloor, A. M.; Ismail, A. A review on RO membrane technology: Developments and challenges. *Desalination* **2015**, *368*, 10−26.
(4) Antony, A.; Low, J. H.; Gray, S.; Childress, A. E.; Le-Clech, P.; Leslie, G. Scale formation and control in high pressure membrane water treatment systems: A review. *J. Membr. Sci.* **2011**, *383* (1), 1−16.
(5) Jiang, S. X.; Li, Y. N.; Ladewig, B. P. A review of reverse osmosis membrane fouling and control strategies. *Sci. Total Environ.* **2017**, *595*, 567−583.
(6) Tong, T.; Elimelech, M. The global rise of zero liquid discharge for wastewater management: Drivers, technologies, and future directions. *Environ. Sci. Technol.* **2016**, *50* (13), 6846−6855.
(7) Tong, T. Z.; Wallace, A. F.; Zhao, S.; Wang, Z. Mineral scaling in membrane desalination: Mechanisms, mitigation strategies, and feasibility of scaling-resistant membranes. *J. Membr. Sci.* **2019**, *579*, 52−69.
(8) Shirazi, S.; Lin, C.-J.; Chen, D. Inorganic fouling of pressure-driven membrane processes—A critical review. *Desalination* **2010**, *250* (1), 236−248.
(9) Rahardianto, A.; McCool, B. C.; Cohen, Y. Reverse osmosis desalting of inland brackish water of high gypsum scaling propensity: kinetics and mitigation of membrane mineral scaling. *Environ. Sci. Technol.* **2008**, *42* (12), 4292−4297.
(10) Karabelas, A.; Karanasiou, A.; Mitrouli, S. Incipient membrane scaling by calcium sulfate during desalination in narrow spacer-filled channels. *Desalination* **2014**, *345*, 146−157.
(11) Lin, N. H.; Kim, M. M.; Lewis, G. T.; Cohen, Y. Polymer surface nano-structuring of reverse osmosis membranes for fouling resistance and improved flux performance. *J. Mater. Chem.* **2010**, *20* (22), 4642−4652.
(12) Van Wagner, E. M.; Sagle, A. C.; Sharma, M. M.; La, Y.-H.; Freeman, B. D. Surface modification of commercial polyamide desalination membranes using poly (ethylene glycol) diglycidyl ether to enhance membrane fouling resistance. *J. Membr. Sci.* **2011**, *367* (1−2), 273−287.
(13) Kang, G. D.; Cao, Y. M. Development of antifouling reverse osmosis membranes for water treatment: A review. *Water Res.* **2012**, *46* (3), 584−600.
(14) Choudhury, R. R.; Gohil, J. M.; Mohanty, S.; Nayak, S. K. Antifouling, fouling release and antimicrobial materials for surface modification of reverse osmosis and nanofiltration membranes. *J. Mater. Chem. A* **2018**, *6* (2), 313−333.
(15) Jhaveri, J. H.; Murthy, Z. A comprehensive review on anti-fouling nanocomposite membranes for pressure driven membrane separation processes. *Desalination* **2016**, *379*, 137−154.
(16) Kim, A.; Hak Kim, J.; Patel, R. Modification strategies of membranes with enhanced Anti-biofouling properties for wastewater Treatment: A review. *Bioresour. Technol.* **2022**, *345*, No. 126501.
(17) Zhang, R.; Liu, Y.; He, M.; Su, Y.; Zhao, X.; Elimelech, M.; Jiang, Z. Antifouling membranes for sustainable water purification: strategies and mechanisms. *Chem. Soc. Rev.* **2016**, *45* (21), 5888−5924.
(18) Kim, M.-m.; Lin, N. H.; Lewis, G. T.; Cohen, Y. Surface nano-structuring of reverse osmosis membranes via atmospheric pressure plasma-induced graft polymerization for reduction of mineral scaling propensity. *J. Membr. Sci.* **2010**, *354* (1−2), 142−149.
(19) Ray, J. R.; Wong, W.; Jun, Y.-S. antiscaling efficacy of CaCO3 and CaSO4 on polyethylene glycol (PEG)-modified reverse osmosis membranes in the presence of humic acid: interplay of membrane surface properties and water chemistry. *Phys. Chem. Chem. Phys.* **2017**, *19* (7), 5647−5657.
(20) Jaramillo, H.; Boo, C.; Hashmi, S. M.; Elimelech, M. Zwitterionic coating on thin-film composite membranes to delay gypsum scaling in reverse osmosis. *J. Membr. Sci.* **2021**, *618*, No. 118568.
(21) Park, S.; Saavedra, M.; Liu, X.; Li, T.; Anger, B.; Tong, T. A comprehensive study on combined organic fouling and gypsum scaling in reverse osmosis: Decoupling surface and bulk phenomena. *J. Membr. Sci.* **2024**, *694*, No. 122399.
(22) Zhu, L.-P.; Jiang, J.-H.; Zhu, B.-K.; Xu, Y.-Y. Immobilization of bovine serum albumin onto porous polyethylene membranes using strongly attached polydopamine as a spacer. *Colloids Surf., B* **2011**, *86* (1), 111−118.
(23) Lee, H.; Dellatore, S. M.; Miller, W. M.; Messersmith, P. B. Mussel-inspired surface chemistry for multifunctional coatings. *Science* **2007**, *318* (5849), 426−430.
(24) Jeong, N.; Wiltse, M. E.; Boyd, A.; Blewett, T.; Park, S.; Broeckling, C.; Borch, T.; Tong, T. Efficacy of nanofiltration and reverse osmosis for the treatment of oil-field produced water intended for beneficial reuse. *ACS ES&T Engineering* **2023**, *3* (10), 1568−1581.
(25) Maruyama, T.; Katoh, S.; Nakajima, M.; Nabetani, H.; Abbott, T. P.; Shono, A.; Satoh, K. FT-IR analysis of BSA fouled on ultrafiltration and microfiltration membranes. *J. Membr. Sci.* **2001**, *192* (1−2), 201−207.
(26) Sukumaran, S. Protein secondary structure elucidation using FTIR spectroscopy. *Thermo Fisher Scientific* **2017**.
(27) Quay, A. N.; Tong, T. Z.; Hashmi, S. M.; Zhou, Y.; Zhao, S.; Elimelech, M. Combined organic fouling and inorganic scaling in reverse osmosis: Role of protein-silica interactions. *Environ. Sci. Technol.* **2018**, *52* (16), 9145−9153.
(28) Ashfaq, M. Y.; Al-Ghouti, M. A.; Da'na, D. A.; Qiblawey, H.; Zouari, N. Effect of concentration of calcium and sulfate ions on gypsum scaling of reverse osmosis membrane, mechanistic study. *Journal of Materials Research and Technology* **2020**, *9* (6), 13459−13473.
(29) Rabizadeh, T.; Peacock, C. L.; Benning, L. G. Investigating the effectiveness of phosphonate additives in hindering the calcium sulfate dihydrate scale formation. *Ind. Eng. Chem. Res.* **2020**, *59* (33), 14970−14980.
(30) Park, J. H.; Jackman, J. A.; Ferhan, A. R.; Ma, G. J.; Yoon, B. K.; Cho, N.-J. Temperature-induced denaturation of BSA protein molecules for improved surface passivation coatings. *ACS Appl. Mater. Interfaces* **2018**, *10* (38), 32047−32057.
(31) Haque, M. A.; Adhikari, B. Drying and denaturation of proteins in spray drying process. *Handbook of industrial drying*, CRC Press: United States, 2015; Vol. 33, pp 971−985.
(32) Baron, F.; Nau, F.; Guérin-Dubiard, C.; Bonnassie, S.; Gautier, M.; Andrews, S. C.; Jan, S. Egg white versus Salmonella Enteritidis! A harsh medium meets a resilient pathogen. *Food Microbiol.* **2016**, *53*, 82−93.
(33) Lajnaf, R.; Feki, S.; Attia, H.; Ali Ayadi, M.; Masmoudi, H. Characteristics of cow milk proteins and the effect of processing on their allergenicity. *Milk protein-New Research approaches*, 2022.
(34) Ruseska, I.; Fresacher, K.; Petschacher, C.; Zimmer, A. Use of protamine in nanopharmaceuticals—A review. *Nanomaterials* **2021**, *11* (6), 1508.


https://doi.org/10.1021/acsenvironau.4c00057
ACS Environ. Au 2024, 4, 333−343

(35) Celik, Y.; Drori, R.; Pertaya-Braun, N.; Altan, A.; Barton, T.; Bar-Dolev, M.; Groisman, A.; Davies, P. L.; Braslavsky, I. Microfluidic experiments reveal that antifreeze proteins bound to ice crystals suffice to prevent their growth. *Proc. Natl. Acad. Sci. U. S. A.* **2013**, *110* (4), 1309−1314.
(36) Garnham, C. P.; Campbell, R. L.; Davies, P. L. Anchored clathrate waters bind antifreeze proteins to ice. *Proc. Natl. Acad. Sci. U. S. A.* **2011**, *108* (18), 7363−7367.
(37) Benecke, J.; Rozova, J.; Ernst, M. Anti-scale effects of select organic macromolecules on gypsum bulk and surface crystallization during reverse osmosis desalination. *Sep. Purif. Technol.* **2018**, *198*, 68−78.
(38) Cao, T.; Rolf, J.; Wang, Z.; Violet, C.; Elimelech, M. Distinct impacts of natural organic matter and colloidal particles on gypsum crystallization. *Water Res.* **2022**, *218*, No. 118500.
(39) Liu, Y. L.; Mi, B. X. Effects of organic macromolecular conditioning on gypsum scaling of forward osmosis membranes. *J. Membr. Sci.* **2014**, *450*, 153−161.
(40) Eickhoff, L.; Dreischmeier, K.; Zipori, A.; Sirotinskaya, V.; Adar, C.; Reicher, N.; Braslavsky, I.; Rudich, Y.; Koop, T. Contrasting behavior of antifreeze proteins: Ice growth inhibitors and ice nucleation promoters. *J. Phys. Chem. Lett.* **2019**, *10* (5), 966−972.
(41) Yan, Z. S.; Qu, F. S.; Liang, H.; Yu, H. R.; Pang, H. L.; Rong, H. W.; Fan, G. D.; Van der Bruggen, B. Effect of biopolymers and humic substances on gypsum scaling and membrane wetting during membrane distillation. *J. Membr. Sci.* **2021**, *617*, No. 118638.
(42) Tong, T.; Park, S.; Yao, Y. A tale of two minerals: contrasting behaviors and mitigation strategies of gypsum scaling and silica scaling in membrane desalination. *Front. Environ. Sci. Eng.*, **2024**.


https://doi.org/10.1021/acsenvironau.4c00057
*ACS Environ. Au* 2024, 4, 333−343